Bioorganic & Medicinal Chemistry 21 (2013) 6337–6348

Contents lists available at ScienceDirect

Bioorganic & Medicinal Chemistry

journal homepage: www.elsevier.com/locate/bmc

Synthesis and anti-*Trypanosoma cruzi* activity of naphthoquinone-containing triazoles: Electrochemical studies on the effects of the quinoidal moiety

Emilay B. T. Diogo [a], Gleiston G. Dias [a], Bernardo L. Rodrigues [a], Tiago T. Guimarães [b], Wagner O. Valença [c], Celso A. Camara [c], Ronaldo N. de Oliveira [c], Mauro G. da Silva [d], Vitor F. Ferreira [e], Yen Galdino de Paiva [f], Marilia O. F. Goulart [f], Rubem F. S. Menna-Barreto [g], Solange L. de Castro [g], Eufrânio N. da Silva Júnior [a,*]

[a] *Instituto de Ciências Exatas, Departamento de Química, UFMG, 31270-901 Belo Horizonte, MG, Brazil*
[b] *Núcleo de Pesquisas de Produtos Naturais, UFRJ, 21941-971 Rio de Janeiro, RJ, Brazil*
[c] *Departamento de Ciências Moleculares, UFRPE, 52171-900 Recife, PE, Brazil*
[d] *Universidade Federal de Pernambuco, UFPE, 50670-901 Recife, PE, Brazil*
[e] *Instituto de Química, UFF, 24020-150 Niterói, RJ, Brazil*
[f] *Instituto de Química e Biotecnologia, UFAL, Tabuleiro do Martins, 57072-970 Maceió, AL, Brazil*
[g] *Laboratório de Biologia Celular, IOC, FIOCRUZ, 21045-900 Rio de Janeiro, RJ, Brazil*

ARTICLE INFO

Article history:
Received 15 June 2013
Revised 18 August 2013
Accepted 26 August 2013
Available online 6 September 2013

Keywords:
Lapachol
β-Lapachone
Quinone
Chagas disease
Trypomastigote
Click chemistry
Electrochemical parameters

ABSTRACT

In our continued search for novel trypanocidal compounds, twenty-six derivatives of *para*- and *ortho*-naphthoquinones coupled to 1,2,3-triazoles were synthesized. These compounds were evaluated against the infective bloodstream form of *Trypanosoma cruzi*, the etiological agent of Chagas disease. Compounds **17**–**24**, **28**–**30** and **36**–**38** are described herein for the first time. Three of these novel compounds (**28**–**30**) were found to be more potent than the standard drug benznidazole, with IC_{50}/24 h values between 6.8 and 80.8 μM. Analysis of the toxicity to heart muscle cells led to LC_{50}/24 h of <125, 63.1 and 281.6 μM for **28**, **29** and **30**, respectively. Displaying a selectivity index of 34.3, compound **30** will be further evaluated in vivo. The electrochemical properties of selected compounds were evaluated in an attempt to find correlations with trypanocidal activity, and it was observed that more electrophilic quinones were generally more potent.

1. Introduction

Chagas disease (CD) is caused by the protozoan *Trypanosoma cruzi* and affects approximately eight million individuals in Latin America. Approximately 30–40% of these patients have, or will develop, cardiomyopathy, digestive mega-syndromes, or both.[1] Although vectorial (*Triatoma infestans*) and transfusional transmission of CD have declined steadily as a result of multinational initiatives,[2] this disease can also be orally transmitted through the ingestion of food or liquid contaminated with *T. cruzi*. This route of transmission is the cause of regional outbreaks of acute infection in areas devoid of domiciled insect vectors.[3] Several outbreaks of severe acute CD, each numbering in the hundreds of cases, have been reported in the Amazon Region in recent decades.[4] Most of these outbreaks were the result of oral transmission. The emergence of CD in non-endemic areas, such as North America and Europe, is another major concern. This development is due to the immigration of infected individuals and subsequent transmission via the blood, organ transplantation and congenital routes.[5,6] Other challenges remaining to be overcome in the fight against CD include the development of sustainable public health policies, vector control strategies and educational approaches.[7,8]

CD is characterized by a short acute phase defined by patent parasitemia followed by a long and progressive chronic phase. Up to 40–50% of chronically infected patients develop progressive cardiomyopathy, motility disturbances of the esophagus and colon, or all of these symptoms. CD is the most severe parasitic infection of the heart, which is the organ most often affected in chronic patients.[1] The available chemotherapy for CD is not satisfactory and depends on two nitroheterocyclic agents: the 5-nitrofuran nifurtimox and the 2-nitroimidazole benznidazole. These compounds are effective against acute infections, but they show poor activity in the later chronic phase. These drugs also cause severe off-target

* Corresponding author. Tel.: +55 31 34095720; fax: +55 31 34095700.
E-mail address: eufranio@ufmg.br (E.N. da Silva Júnior).

0968-0896/$ - see front matter © 2013 Elsevier Ltd. All rights reserved.
http://dx.doi.org/10.1016/j.bmc.2013.08.055

effects, have limited efficacy against different parasite isolates and must be applied in long-term therapy. These drawbacks justify the urgent effort to identify better drugs for the treatment of CD.[9,10] Nearly all current drug development efforts for CD are in the pre-clinical research phase, although Phase II clinical trials with the antifungal drug posaconazole are underway in Latin America and Spain. A ravuconazole prodrug is also undergoing Phase II studies in Bolivia.[11]

Plants represent a vast reservoir of phytoconstituents and secondary metabolites that can be used as templates for the design of semi-synthetic or synthetic compounds. This approach can lead to the discovery of new candidates for the treatment of neglected tropical diseases with high therapeutic indices. Naphthoquinones account for the majority of naturally occurring naphthalenes,[12] displaying an assortment of substituents over a variety of structural motifs. They act as vital links in the electron transport chains of metabolic pathways and participate in multiple biologically relevant oxidative processes.[13]

Naphthoquinones are considered privileged scaffolds in medicinal chemistry due to their structural properties and biological activities,[14] especially against tumor cells and pathogenic protozoa.[15] We have recently described the synthesis and trypanocidal and leishmanicidal activities of 1,2,3-triazoles based on the lapachone scaffold.[16,17a] Modification of the prototype β-lapachone, as shown in Scheme 1, is a relevant strategy for the development of novel bioactive compounds. The C-ring was modified to afford nor-β-lapachone and β-lapachone derivatives with pronounced activity against trypomastigote forms of *T. cruzi*.[16] Other derivatives can be prepared by modification of the redox centre and the C-ring, as described in Scheme 1: arylamino derivatives of nor-β-lapachone, imidazoles and oxiranes are important examples of this strategy.[16–18] Recently, nor-α-lapachone and α-lapachone derivatives were also prepared and shown to have potent activity against promastigote forms of antimony-sensitive and -resistant strains of *Leishmania infantum* (syn. *L. chagasi*) and *L. amazonensis*.[17a]

Several studies have investigated and reported the electrochemical behavior of quinones. Some correlation has been demonstrated between electrochemical parameters and disease states.[19] The quinone/semiquinone/hydroquinone ($Q/SQ^{\bullet-}/H_2Q$) triad is an important component of many redox systems in biology. It is a vital link in the transfer of electrons through cells and tissues (Eqs. 1–3).[20]

$$Q + e^- \rightleftharpoons SQ^{\bullet-} \quad (1)$$

$$SQ^{\bullet-} + e^- + 2H^+ \rightleftharpoons H_2Q \quad (2)$$

$$\text{Net} \quad Q + 2e^- + 2H^+ \rightleftharpoons H_2Q \quad (3)$$

Electrochemical techniques have been used extensively to provide excellent insights into the modes of action of various drugs, and these results can inspire the design of next-generation therapeutics. This approach is particularly suitable for diseases associated with cellular oxidative stress, which is a hallmark of cancer.[19–21] Electrochemistry experiments can provide data on the fundamental thermodynamic and kinetic properties associated with the reactions of quinones and reduced intermediates.

The versatility and functional diversity of quinones are due primarily to the diverse mid-point potentials that are sensitive to substituent effects, solvent and medium effects (hydrophilic/lipophilic) and interactions with certain macromolecules (e.g., DNA and proteins). The electronic properties of quinones are influenced by substituent groups, hydrogen bonding (H-bonding), hydrophobic and π-stacking interactions and conformational effects. These factors act in tandem to stabilize or destabilize the semiquinone radical (under aprotic conditions or during enzymatic one-electron transfer). They can be correlated to the nature of the anion radical that is formed in vivo or to the completely reduced species (hydroquinones or modified derivatives).[19b,21]

In this context, we herein describe the synthesis of *para*- and *ortho*- naphthoquinones bearing 1,2,3-triazole substituents, as well as 1,2,3-triazoles derived from α-lapachone and nor-α-lapachone. These compounds were evaluated for activity against trypomastigote forms of *T. cruzi*. Electrochemical studies of selected compounds are also presented.

Our synthetic rationale was to combine *para* and *ortho* quinoidal moieties with heterocycles (Schemes 2–4). Derivatives of *N*-phthalimide have been shown to have biological significance, including antibacterial,[22] antiviral,[23] anticancer[24] and anti-hepatitis activity.[25] Based on the pharmacological importance of phthalimide analogues, we synthesized hybrids of 1,4-naphthoquinone and *N*-phthalimide conjugated through an aminomethyl-triazole linkage. The introduction of a second quinoidal moiety was also accomplished (Scheme 4) in a hybrid approach to duplicate the effect of the quinone. Finally, the importance of the redox centre was analyzed by modifying the structure of

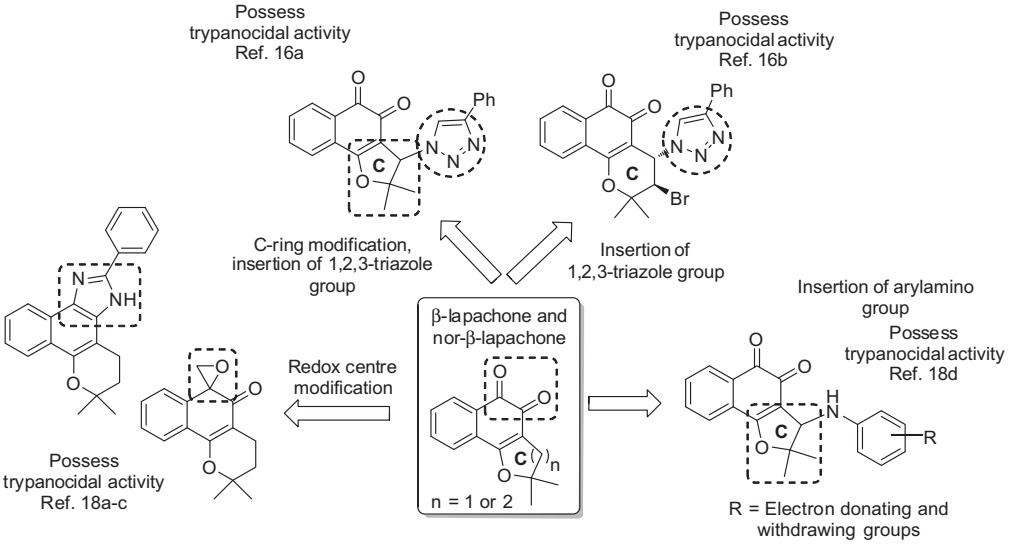

Scheme 1. Structural modification of the prototype β-lapachone and nor-β-lapachone.

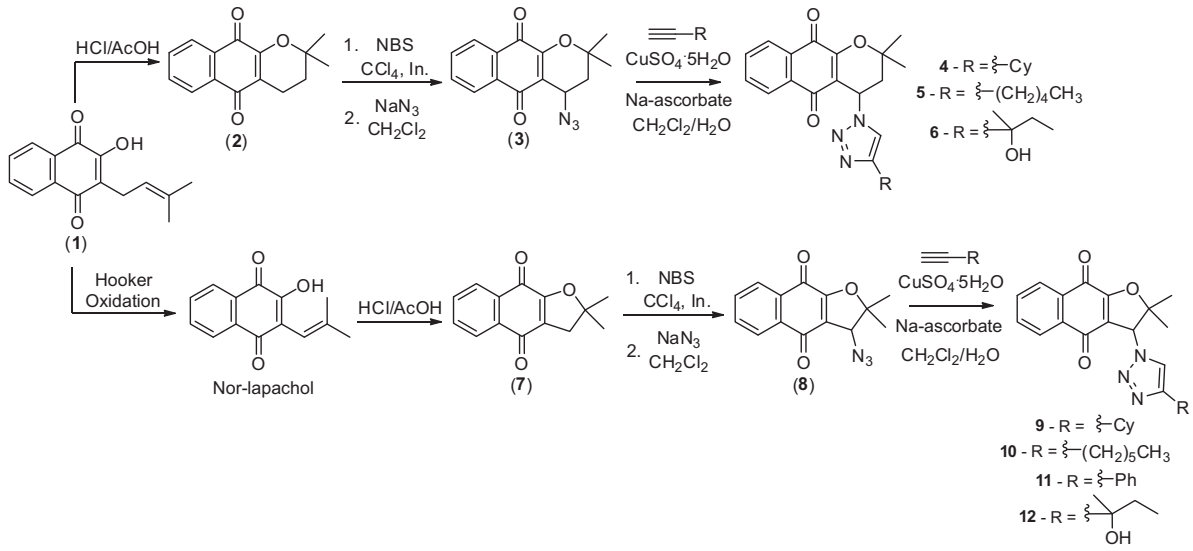

Scheme 2. α-Lapachone- and nor-α-lapachone-derived 1,2,3-triazoles **4**–**6** and **9**–**12**.

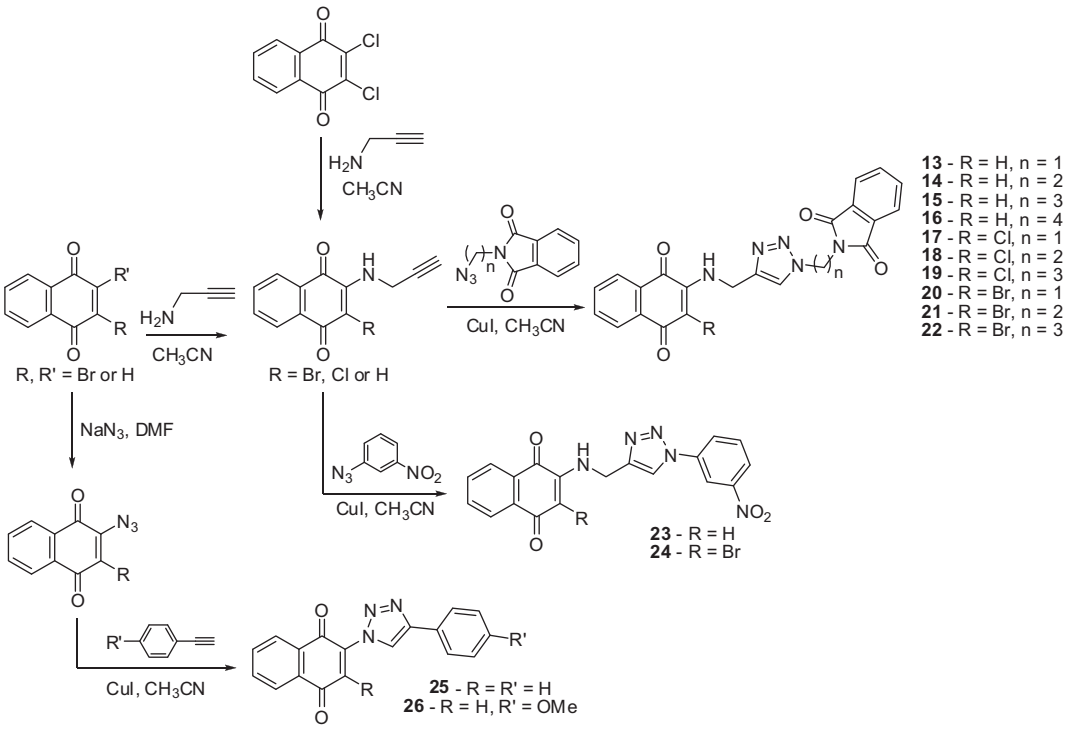

Scheme 3. 1,4-Naphthoquinone-derived 1,2,3-triazoles **13**–**26**.

nor-β-lapachone-based 1,2,3-triazole to generate compounds similar to phenazine derivatives (Scheme 5).

2. Results and discussion

2.1. Chemistry

α-Lapachone and nor-α-lapachone-derived 1,2,3-triazoles were synthesized as described previously (Scheme 2).[17a] Lapachol (**1**) was used to prepare α-lapachone (**2**), which was subsequently treated with *N*-bromosuccinimide in carbon tetrachloride, in the presence of benzoyl peroxide, to provide 4-bromo-α-lapachone. This bromide was reacted with sodium azide to yield 4-azido-α-lapachone (**3**). The 1,2,3-triazoles **4**–**6** were then obtained from Cu(I)-catalyzed reactions with the appropriate alkynes, following the methodology described by Sharpless and co-workers (Scheme 2).[17b]

Lapachol (**1**) was used to prepare nor-lapachol in two steps as described previously.[26] This derivative was treated with HCl/AcOH to provide nor-α-lapachone (**7**). Conversion to 3-bromo-nor-α-lapachone and reaction with sodium azide in dichloromethane gave the corresponding azide **8**, as described previously.[17a] Triazole derivatives **9**–**12** were synthesized from quinone **8** (Scheme 2).

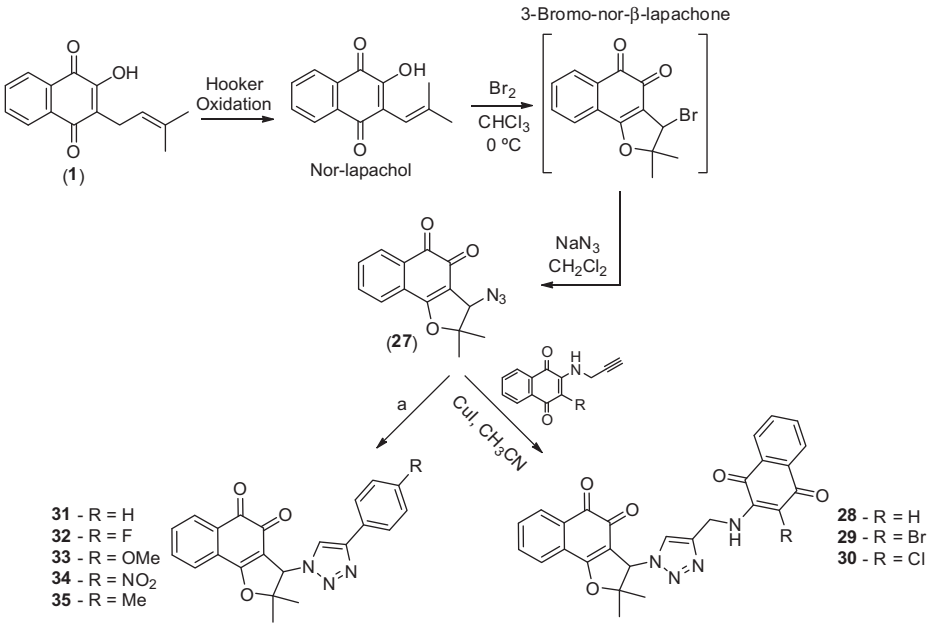

Scheme 4. Nor-β-lapachone-derived 1,2,3-triazoles **28**–**35**. (a) Ref. 16a,d.

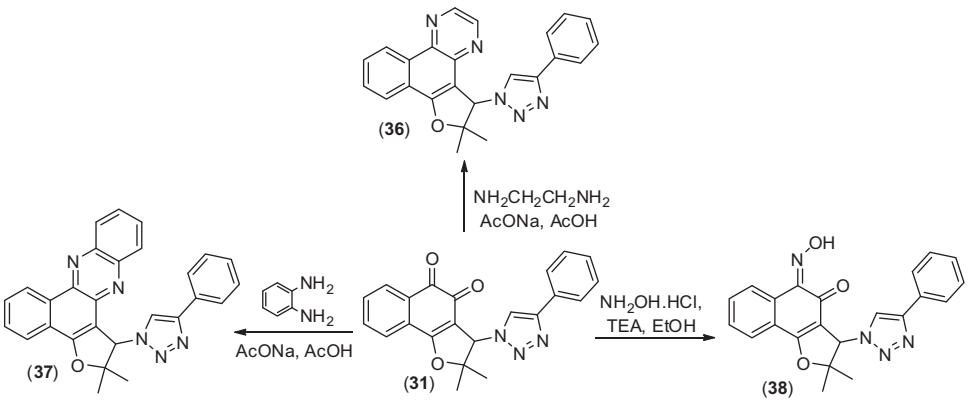

Scheme 5. Preparation of 1,2,3-triazoles **36**–**38** derived from nor-β-lapachone based on compound **31**.

A previously described methodology[16d,27] was used to prepare *para*-naphthoquinones **13**–**26** (Scheme 3). A series of *N*-phthalimidoalkylazides was initially prepared for the synthesis of compounds **13**–**22**. These intermediates were used in click chemistry reactions with substituted 2-(prop-2-yn-1-ylamine)-naphthoquinone to obtain the respective triazole compounds in high yields. Compounds **23** and **24** were prepared by the click reaction among the respective quinone and 1-azido-3-nitrobenzene. Final compounds were typically isolated as crystalline solids, and all spectroscopic data were in accordance with the proposed structures shown in Scheme 3. Compounds **17**–**24** are described herein for the first time.

The last set of naphthoquinoidal compounds was synthesized from the intermediate azide **27** that we have described previously.[16a] Naphthoquinones substituted with a terminal alkyne had been synthesized previously. These compounds were subjected to click chemistry conditions[17b] to prepare novel derivatives **28**–**30** as shown in Scheme 4. Nor-β-lapachone derivatives **28**–**30** were isolated in moderate yields as yellow and orange solids. Known compounds **31**–**35**,[16a,d] shown in Scheme 4, were included to study their electrochemical properties in comparison with their trypanocidal activity (vide infra).

Cu-Catalyzed Azide-Alkyne Cycloaddition (CuAAC) is a well established methodology using Cu(I) as source of catalysis.[28] Herein, we described the synthesis of quinone-based 1,2,3-triazoles using two reaction conditions, the most common using aqueous conditions employing $CuSO_4{\cdot}5H_2O$ and sodium ascorbate as reducing agent and copper(I) iodide in acetonitrile. As recently described by Meldal and Tornøe[29] there is no obvious correlation between method used and yield of reaction. In general, $CuSO_4{\cdot}5H_2O$ and sodium ascorbate is preferred due to ease of workup, while, in other reactions, the copper(I) iodide can be used to improve the rate of reaction. In this manuscript the classical methodology published by Sharpless and co-workers[17b] was used preferentially. In the case of low yields and long reaction time, copper(I) iodide in acetonitrile or the same condition under ultrasound energy were used.

The phenyl substituted 1,2,3-triazole derived from nor-β-lapachone (**31**) was described previously and was shown to be sixfold more potent than the standard drug benznidazole against trypomastigote forms of *T. cruzi*.[16a] Herein we describe

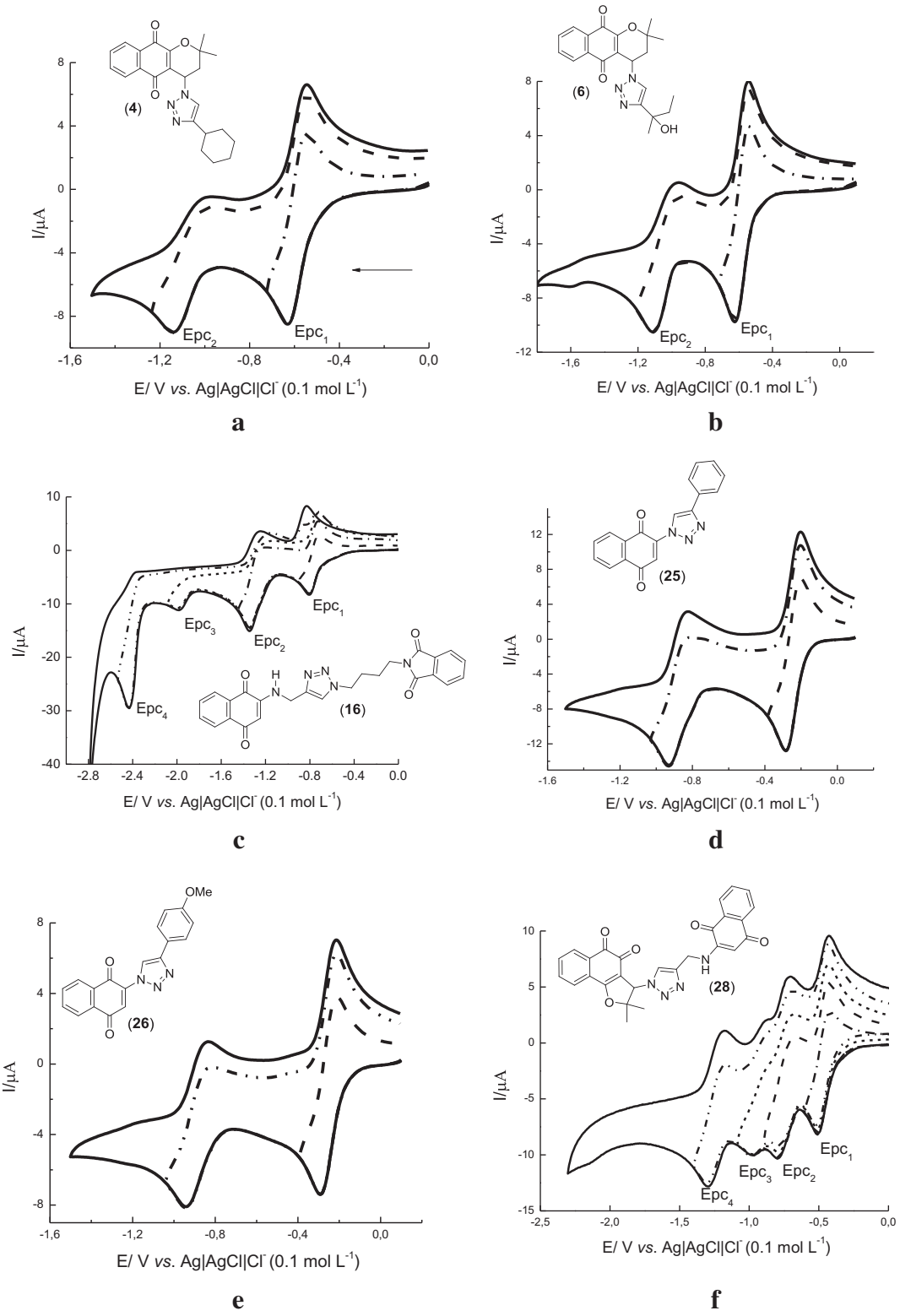

Figure 1. Cyclic voltammograms of naphthoquinones **4**, **6**, **9**, **16**, **25**, **26**, **28**, **30**–**35** ($c = 1 \times 10^{-3}$ mol L^{-1}). DMF/TBAP (0.1 mol L^{-1}), glassy carbon electrode, cathodic direction, $v = 50$ mV.

the synthesis of three novel derivatives synthesized from **31** (Scheme 5). Our strategy was based on modifying the redox centre of **31**. We selected modification reactions from previously published studies on related β-lapachone derivatives, which showed pronounced activity against *T. cruzi*.[16] Compound **31** was obtained in five steps, in good overall yield, starting from lapachol (**1**).[16a] Intermediate **31** reacted smoothly with ethane-1,2-diamine or *ortho*-phenylenediamine in acetic acid[30] to furnish compounds

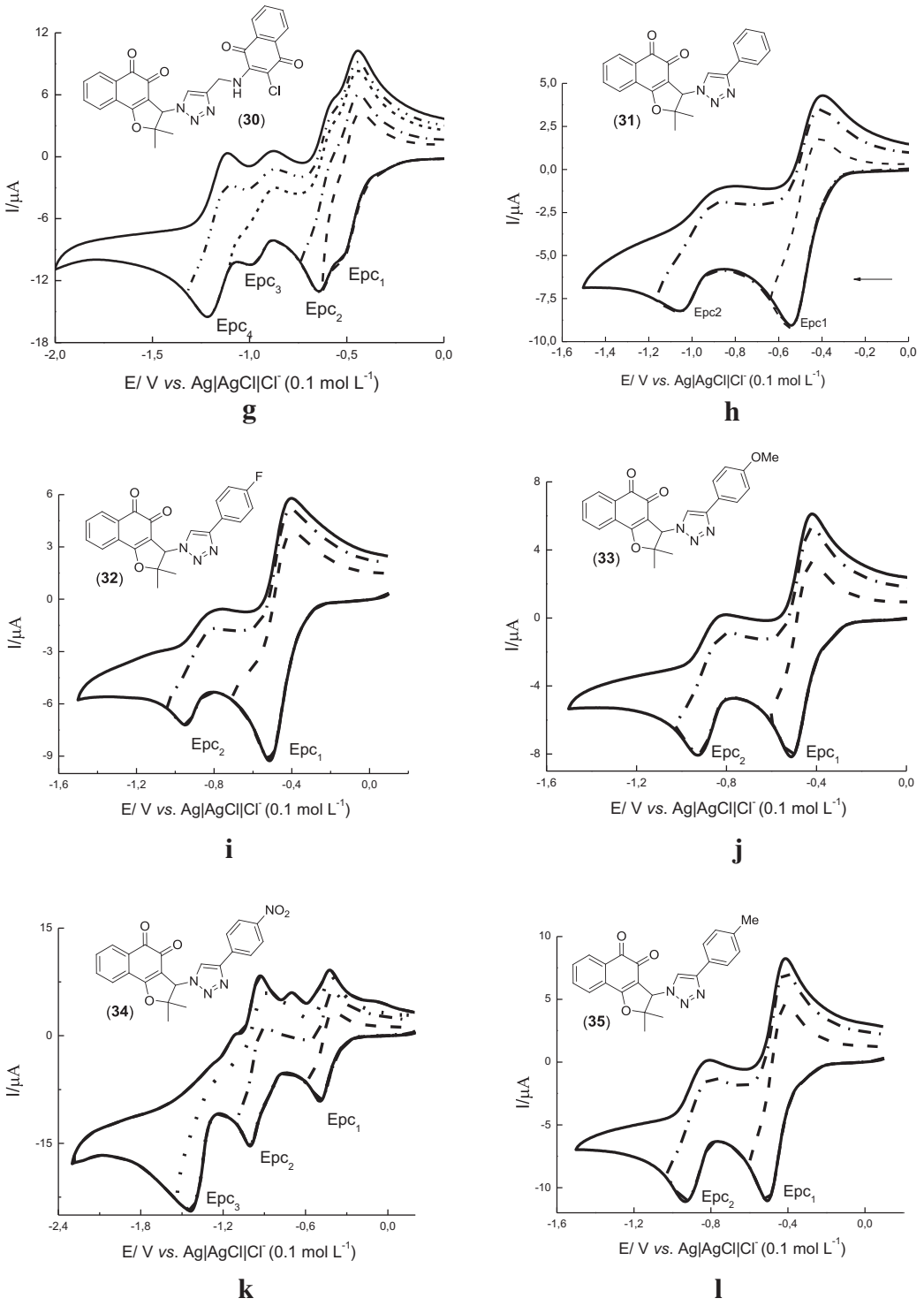

Fig. 1 (*continued*)

36 and **37** in excellent yields. Oxime **38** was prepared by reaction of **31** with hydroxylamine in ethanol in the presence of TEA (Scheme 5).[31]

The structures of novel compounds **17**–**24**, **28**–**30** and **36**–**38** were determined by ^{1}H, ^{13}C NMR, and IR. The structures were further characterized by comparing their spectroscopic data with those of similar compounds known in the literature.[16a,17a,18] Electrospray ionization mass spectra and combustion analysis data were also obtained. Crystals of **38** suitable for X-ray analysis were obtained, and the structure was solved. ORTEP-3 projections are shown in Figure 2, and these reveal the *Z*-stereochemistry.

2.2. Electrochemistry

In a typical measurement, cyclic voltammograms (CV) were recorded first in aprotic medium (DMF + TBAP, 0.1 mol L^{-1}), at a scan

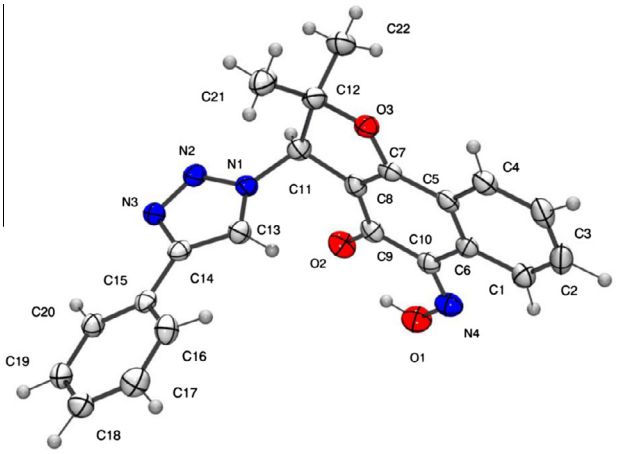

Figure 2. ORTEP-3 projection of compound **38** showing atom labeling and displacement ellipsoids drawn at the 50% probability level.

Table 1
Major electrochemical parameters of the quinones ($c = 1 \times 10^{-3}$ mol L^{-1}), in DMF/TBAP, 0.1 mol L^{-1}, $\nu = 50$ mV s^{-1}

Compound	Epc1 (V)	E_{redox} (V)	Epc2 (V)	Additional waves (V)
4	−0.630	−0.586	−1.143	–
6	−0.623	−0.581	−1.110	–
16	−0.807	−0.761	−1.348	−1.993, −2.436
25	−0.286	−0.244	−0.930	–
26	−0.291	−0.252	−0.940	–
28	−0.511	−0.467	−0.799	−0.965, −1.311
30	−0.521	−0.475	−0.648	−0.999, −1.216
31	−0.535	−0.472	−1.055	–
32	−0.515	−0.454	−0.950	–
33	−0.510	−0.464	−0.925	–
34	−0.493	−0.444	−1.001	−1.441
35	−0.506	−0.457	−0.935	–

rate of 50 mV s^{-1}. This enabled determination of the electrochemical reduction behavior of each compound. Initial cathodic and anodic peak currents were also determined for each compound.

It was not feasible to study all of the quinones in the present work. Representative compounds were selected to cover each of the structural classes (Schemes 2–4).

As has been noted, the compounds described here can be divided among three structural classes: dihydropyran-*para*-naphthoquinones (**4** and **6**), *para*-naphthoquinone derivatives (**16**, **25** and **26**), and *ortho*-dihydrofuranones (**28**, **30**–**35**).

Figure 1 shows the cyclic voltammograms of compounds **4**, **6**, **16**, **25**, **26**, **28**, and **30**–**35**. All of the quinones exhibited quasi-reversible reduction behavior (Fig. 1). The major electrochemical parameters for each compound are listed in Table 1.

The relative ease of reduction among the compounds was established by comparison of their first reduction potentials (Epc1, Table 1, column 2). The relative reduction potential of the compounds is as follows: **25** > 26 > **34** > **35** > **33** > **28** ~ **32** ~ **30** > **31** > **6** ~ **4** > **16**.

The values of E_{redox} were obtained from the equation (Epc1 + Epa1)/2 and are shown in Table 1. As was expected for quinonoid compounds, the overall CV profiles are similar to those reported for other quinones. The characteristic profile shows two couples of cathodic and anodic peaks, represented by diffusional (Eplc α $\nu^{1/2}$) quasi-reversible systems.[19b,c] The first pair is related to the formation of a radical anion ($SQ^{\bullet-}$, Eq. (1)). The second pair of peaks is broader and ill-defined, as has been observed previously.[19b] This broadening may be due to possible disproportionation or comproportionation reactions.[19b]

As shown in Table 1, compounds **25** and **26** (Fig. 1d and e) are most easily reduced. The direct attachment of the electron-withdrawing triazole affects the electrochemical behavior of the *para*-quinones in a way that facilitates electron transfer. On the other hand, the presence of an electron-donating amine group increases the barrier to reduction of compound **16** (Fig. 1c). This compound presents two additional waves at more negative potentials (Epc3 and Epc4, Fig. 1c, Table 1, column 4). A full description of the electrodic mechanism is beyond the scope of the present paper and will be described elsewhere. It is noticeable that nor-β-lapachone *ortho*-quinones derivatives (**31**–**35**, Fig. 1h–l) are more easily reduced than are the α-lapachone-derived 1,2,3-triazoles (**4** and **6**, Fig. 1a and b), as has been shown previously.[19b] The CV of compound **34**, which shows the lowest negative potential in this series,

Table 2
Crystal data and structure refinement for compound **38**

Empirical formula	$C_{22}H_{18}N_4O_3$	
Formula weight	386.41	
Temperature	150(2) K	
Wavelength	0.71073 Å	
Crystal system, space group	Monoclinic, $P2_1$	
Unit cell dimensions	$a = 5.6099(2)$ Å	$\alpha = 90°$
	$b = 11.3548(5)$ Å	$\beta = 96.641(4)°$
	$c = 14.5658(7)$ Å	$\gamma = 90°$
Volume	921.61(7) $Å^3$	
Z, Calculated density	2, 1.392 mg/m^3	
Absorption coefficient	0.095 mm^{-1}	
$F(000)$	404	
Crystal size	0.087 × 0.170 × 0.188 mm^3	
Theta range for data collection	2.28–29.42°	
Limiting indices	−7<=h<=7, −14<=k<=14, −19<=l<=18	
Reflections collected	4789	
Independent reflections	3346 [R(int) = 0.0275]	
Completeness to theta = 26.32°	99.95%	
Absorption correction	Semi-empirical from equivalents	
Max. and min. transmission	1 and 0.93	
Refinement method	Full-matrix least-squares on F^2	
Data/restraints/parameters	3346/1/272	
Goodness-of-fit on F^2	1.107	
Final R ÿ indices [$I > 2\sigma(I)$]	$R_1 = 0.0465$, $wR_2 = 0.1163$	
R indices (all data)	$R_1 = 0.0598$, $wR_2 = 0.1342$	
Largest diff. peak and hole	0.292 and −0.315 e $Å^{-3}$	

Table 3
Intermolecular interaction parameters (A, °) for compound **38**

A-H···B	*d*(A-B)	*d*(A-H)	*d*(H···A)	<(DHA)
C18[1]-H18[1]···N3	3.364(4)	0.963(3)	2.665(2)	129.8(2)
C19[2]-H19[2]···N2	3.297(4)	0.977(3)	2.588(2)	129.51(19)
C13-H13···O2	3.477(3)	0.984(3)	2.527(2)	162.24(19)

Symmetry operators: (1) $-x, -0.5+y, 2-z$; (2) $1-x, -0.5+y, 2-z$; (3) $-1+x, y, z$.

displayed additional waves that can be attributed to an additional electron-withdrawing nitro group (Fig. 1k). The behavior of this compound is characterized by three waves. The first wave arises from single electron transfer to the quinone system. The second is attributable to a combined system, with two close electron transfers: one to the semiquinone and the other to the nitroaromatic group, generating a nitro radical anion. The third wave is related to further reduction of the nitroaromatic system.

The presence of two quinone systems in **28** and **30** (Fig. 1f and g) leads to CV curves displaying considerably more complex features. These curves show at least four cathodic waves and corresponding anodic waves. It is clear from comparison with the CV of compound **16** that the first wave is related to the reduction of the *ortho*-quinone.

2.3. X-ray analysis

The Ortep-3 diagram of **38** is shown in Figure 2, and Table 2 lists the major crystallographic parameters. Compound **38** crystallizes in the non-centrosymmetric space group $P2_1$, with one molecule in the asymmetric unit. The bond lengths and angles are in good agreement with expected values, based on each atomic type. Although the statistical and structural parameters indicate that the structure is well solved, the Flack parameter indicates that the absolute structure cannot be resolved from this analysis. The crystal structure reveals one intramolecular hydrogen bond (O1–H10···O2) that forms a six-membered ring. Three main planes may be defined through the molecule. Plane 1 is formed by the quinoidal ring (atoms C1 to C10, as O1, O2 and N4). It is interesting to note that atoms C11 and O3 of the furan ring are close to plane 1 (distances equal to 0.059(4) Å 0.044(4) A), while atom C12 is more distant from this plane (0.238(5) Å). Plane 2 is formed by atoms N1, N2, N3, C13 and C14. Nitrogen N1 of this plane is bonded to the chiral C11 atom of plane 1. The distance between C11 and plane 2 is equal to 0.018(5) Å, indicating that these atoms belong to both planes. Plane 3 is defined through the benzene ring (atoms C15–C20). The angle between planes 1 and 2 is equal to 85.75(7)°, while the angle between planes 2 and 3 is equal to 18.91(18)°. This suggests that the phenyl ring and the triazole group are approximately coplanar. The crystal packing is stabilized by intermolecular C–H···N and C–H···O interactions, involving atoms C13, N2 and N3 of the triazole ring (Table 3).

2.4. Biological activity

We have recently described the introduction of 1,2,3-triazole and arylamino groups into naphthoquinoidal structures; some of these substances were identified as potent trypanocidal compounds.[16] In that work, we demonstrated that 1,4-naphthoquinones and β-lapachones derivatized with a 1,2,3-triazole had efficacy as novel trypanocidal compounds.

In the present study, we have evaluated four classes of compounds for activity against *T. cruzi*. These include α-(**4**–**6**) and nor-α-lapachone-derived 1,2,3-triazoles (**9**–**12**), aminomethylnaphthoquinones conjugated to *N*-phthalimide via triazole linkers (**13**–**22**), nor-β-lapachone-derived 1,2,3-triazole-conjugated aminoquinones (**28**–**30**) and derivatives of nor-β-lapachone bearing phenazine and oxime moieties (**36**–**38**). Previously published data are included in Table 4 and the associated footnote to enable comparison.[16a,d]

Table 4
Activity of compounds against the trypomastigote form of *T. cruzi*

Compound	IC_{50}/24 h[a] (μM)
Lapachol (**1**)[b]	410.8 ± 53.5
α-Lapachone (**2**)[b]	>4800
4-Azido-α-lapachone (**3**)	318.2 ± 31.8
4	>2000
5	>4000
6	>500
Nor-α-lapachone (**7**)[c]	>4800
3-Azido-nor-α-lapachone (**8**)[c]	179.3 ± 12.0
9	>1500
10	>2000
11	>4000
12	>4000
13	>4000
14	>4000
15	>4000
16	>4000
17	>4000
18	>4000
19	>4000
19	>4000
20	>4000
21	>4000
22	>4000
23	>4000
24	>4000
25[d]	10.9 ± 1.8
26[d]	45.8 ± 5.1
3-Azido-nor-β-lapachone (**27**)[c]	50.2 ± 3.8
28	80.8 ± 6.5
29	6.8 ± 0.7
30	8.2 ± 0.7
31[a]	17.3 ± 2.0
32[c]	20.8 ± 1.9
33[c]	359.2 ± 11.1
34[c]	21.8 ± 3.1
35[c]	39.6 ± 4.0
36	>4000
37	>1500
38	>3200
Benznidazole[c]	103.6 ± 0.6
Crystal violet[c]	536.0 ± 3.0

[a] Mean ± SD of at least three independent experiments.
[b] Ref. 18d.
[c] Ref. 16a.
[d] Ref. 16d.

The first class of compounds, α-lapachones linked to 1,2,3-triazoles (*para*-quinones, Scheme 2), was synthesized from α-lapachone (**2**) and nor-α-lapachone (**7**). We sought to evaluate the effect of the 1,2,3-triazole ring on the trypanocidal activity of these compounds. This strategy had previously been shown to be effective for derivatives of nor-β-lapachone (*ortho*-quinones). Unfortunately, compounds **4**–**6** and **9**–**12** were inactive against trypomastigote forms of *T. cruzi*, with IC_{50}/24 h values greater than 500 μM for all derivatives (Table 4).

The hybrids of 1,4-naphthoquinone and *N*-phthalimide (**13**–**22**) were prepared from brominated, chlorinated or unsubstituted quinones with spacers of one, two or three carbon atoms between the 1,2,3-triazole ring and the *N*-phthalimido group (Scheme 3). Compounds **13**–**22** were inactive against *T. cruzi*, as all showed IC_{50}/24 h values greater than 4000 μM. Compounds **23** and **24** were also inactive (Table 4).

The last class of naphthoquinoidal compounds described herein was designed to couple *ortho*-quinone to *para*-quinoidal structures

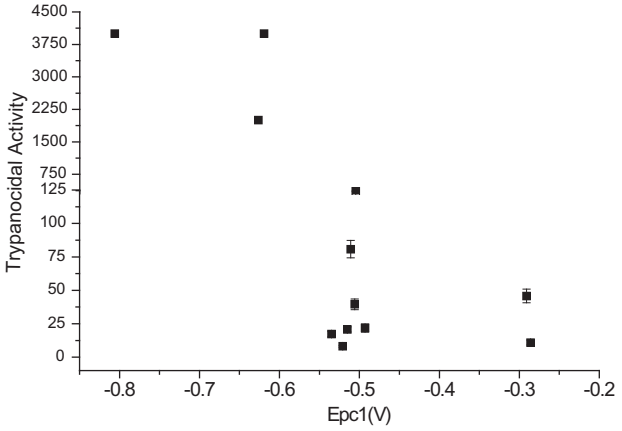

Figure 3. Graph correlating the values of Epc1 of each quinone with its trypanocidal activity (bloodstream trypomastigote forms), represented by IC_{50}/24 h (μM).

(Scheme 4). Compounds **28**–**30** were isolated in moderate yields as yellow and orange crystalline solids. Our approach proved to be effective, and **28**, **29** and **30** showed IC_{50}/24 h values of 80.8, 6.8 and 8.2 μM, respectively (Table 4). The compounds **29** and **30** were about 15 times more potent than benznidazole, the drug used for the treatment of Chagas disease. A hypothesis for the potent trypanocidal activity is that the union of *ortho*- and *para*-quinoidal moieties can generate high concentrations of reactive oxygen species, in general related to activity of this class of compounds. Analysis of the toxicity to heart muscle cells gave the LC_{50}/24 h values of <125, 63.1 and 281.6 μM for **28**, **29** and **30**, respectively, corresponding to selectivity indexes (SI) of <1.5, 9.3 and 34.3. As preconized in the workshop 'Experimental Models in Drug Screening and Development for Chagas Disease' organized by Fiocruz and Drugs for Neglected Diseases Initiative (DNDi)[32] establishing a protocol for drug screening, compound **30** will be submitted to in vivo experiments using *T. cruzi*-infected mice. These results highlight the potential of these compounds as novel trypanocidal agents.

To evaluate the importance of redox centers primarily as releasers of ROS, we prepared a series of compounds by modifying the scaffold of the previously described trypanocidal nor-β-lapachone derivative **31** (Scheme 5).[16a] Compounds **36**–**38** were evaluated against trypomastigote forms of *T. cruzi*, but none were found to be active (Table 4).

A comparison of the data in Tables 1 and 4 (Fig. 3) reveals a trend: more electrophilic quinones, that is, those with less negative values for Epc1, (Epc1 >−0.6 V vs Ag/AgCl, Table 1) were more potent trypanocidal compounds. Compound **33** was the lone exception to this trend.

Electrochemical experiments (analytical and preparative) and electrochemical (thermodynamic and kinetic) parameters are useful in biomedical chemistry, particularly in elucidating the mechanisms of biological electron-transfer processes. Such analyses can be useful in the design of putatively bioactive lead compounds for which the mechanism of action is based on redox reactions leading to oxidative stress.[21a]

3. Conclusions

We evaluated twenty-six compounds, and three were identified as potent trypanocidal agents. These compounds were more active than the anti-*T. cruzi* drug benznidazole, the current therapeutic standard. As compound **30** was 12-fold more active than benznidazole, it is a promising candidate for further investigation. The electrochemical properties of selected compounds were studied, and important correlations were found with trypanocidal activity.

4. Experimental section

4.1. Chemistry

Melting points were obtained on Thomas Hoover and are uncorrected. Analytical grade solvents were used. Column chromatography was performed on silica gel (SiliaFlash G60 UltraPure—60–200 μm, 60 Å). Infrared spectra were recorded on an FTIR Spectrometer IR Prestige-21—Shimadzu. ^{1}H and ^{13}C NMR were recorded at room temperature using a Bruker AVANCE DRX200, Varian Mercury 300 and Varian Mercury 400 MHz, in the solvents indicated, with TMS as internal reference. Chemical shifts (δ) are given in ppm and coupling constants (J) in Hertz. High resolution mass spectra (electrospray ionization) were obtained using a MicroTOFIc—BrukerDaltonics. Elemental analysis was performed using a CE Instruments (Thermo-Fisher) EA 1110 CHNS-O elemental analyzer. All the compounds were nominated using the program CS ChemDraw Ultra version 10.0.

4.2. General procedure for the synthesis of compounds 17–24

Method A: In a flask containing 3 mL acetonitrile, it was added 0.5 mmol of the appropriate azides, followed by 0.6 mmol of the appropriate alkynes and finally 11 mg (0.06 mmol) of copper(I) iodide. The reaction was left under magnetic stirring at 28 °C under argon atmosphere, for a reaction time ranging from 19 to 24 h. The end of the reaction was monitored by TLC with dichloromethane as eluent. The solvent was then removed under reduced pressure and the reaction mixture was purified on a silica gel column as a gradient mixture of hexane/ethyl acetate or dichloromethane/ethyl acetate with increasing polarity. *Method B:* In a flask containing 2 mL of DMF, it was added 0.5 mmol of the appropriate azides, followed by 0.6 mmol of the appropriate alkynes, 11 mg (0.06 mmol) of copper(I) iodide and finally 1 drop of Et_3N. The reaction was left under ultrasound energy at 28 °C, during 30 min. After the end of the reaction monitored by TLC with dichloromethane, the mixture was purified as described in method A. *Method C:* The same procedures described in Method A, but 2 mL DMF, one drop Et_3N were added and the reaction was left under magnetic stirring for 60 min as monitored by TLC. *Method D:* The same procedures described in method A, 2 mL of DMF were added, and the reaction was left under magnetic stirring for 60 min as monitored by TLC.

4.2.1. 2-((4-(((3-Chloro-1,4-dioxo-1,4-dihydronaphthalen-2-yl)amino)methyl)-1*H*-1,2,3-triazol-1-yl)methyl)isoindoline-1,3-dione (17)

Using method D, compound **17** was obtained as an orange solid (200 mg, 0.44 mmol, 87% yield); mp 170–172 °C. IR ν_{max} (cm^{-1}, KBr): 3324, 3140, 2955, 1775, 1712, 1672, 1605, 1573, 1507, 1403, 1363, 1330, 1293, 1136, 1048, 953, 717. ^{1}H NMR (400 MHz, $CDCl_3$) δ: 8.12 (dd, 1H, J = 1.2 and 8.0 Hz), 8.01 (dd, 1H, J = 1.2 and 8.0 Hz), 7.91–7.89 (m, 3H), 7.78–7.76 (m, 2H), 7.70 (td, 1H, J = 1.6 and 7.3 Hz), 7.61 (td, 1H, J = 1.6 and 7.3 Hz), 6.41 (br s, 1H, NH), 6.20 (s, 2H), 5.14 (d, 2H, J = 6.4 Hz). ^{13}C NMR (100 MHz, $CDCl_3$) δ: 177.6, 174.1, 163.8, 142.4, 141.4, 132.4, 132.1, 132.0, 128.8, 127.4, 124.2, 124.1, 121.6, 121.4, 120.5, 120.3, 47.2, 37.6. Anal. Calcd for $C_{22}H_{14}ClN_5O_4$ 0.3 × H_2O: C, 58.30; H, 3.25; N, 15.45. Found: C, 58.48; H, 3.21; N, 15.24.

4.2.2. 2-(2-(4-(((3-Chloro-1,4-dioxo-1,4-dihydronaphthalen-2-yl)amino)methyl)-1*H*-1,2,3-triazol-1-yl)ethyl)isoindoline-1,3-dione (18)

Using method D, compound **18** was obtained as a red solid (200 mg, 0.44 mmol, 71% yield); mp 197–199 °C. IR ν_{max} (cm^{-1},

KBr): 3313, 3141, 1774, 1715, 1678, 1605, 1572, 1525, 1425, 1391, 1356, 1298, 1139, 1049, 943, 720. ^{1}H NMR (400 MHz, $CDCl_3$) δ: 8.15 (d, 1H, J = 7.6 Hz), 8.04 (d, 1H, J = 7.6 Hz), 7.79–7.61 (m, 7H), 6.41 (br s, 1H, NH), 5.13 (d, 2H, J = 5.6 Hz), 4.69 (t, 2H, J = 6.4 Hz), 4.15 (t, 2H, J = 6.0 Hz). ^{13}C NMR (100 MHz, $CDCl_3$) δ: 180.3, 167.5, 134.8, 134.3, 132.6, 131.7, 126.8, 123.6, 48.2, 40.3, 37.7. Anal. Calcd for $C_{23}H_{16}ClN_5O_4$ 0.35 × H_2O: C, 59.01; H, 3.49; N, 15.16. Found: C, 59.38; H, 3.64; N, 14.56.

4.2.3. 2-(3-(4-(((3-Chloro-1,4-dioxo-1,4-dihydronaphthalen-2-yl)amino)methyl)-1*H*-1,2,3-triazol-1-yl)propyl)isoindoline-1,3-dione (19)

Using method D, compound **19** was obtained as a red solid (200 mg, 0.44 mmol, 94% yield); mp 179–181 °C. IR ν_{max} (cm^{-1}, KBr): 3313, 3141, 1774, 1712, 1678, 1602, 1571, 1525, 1435, 1293, 1139, 1049, 716. ^{1}H NMR (400 MHz, acetone-d_6) δ: 7.93–7.60 (m, 2H), 7.70–7.61 (m, 7H), 6.94 (br s, 1H, NH), 5.01 (d, 2H, J = 5.9 Hz), 4.37 (t, 2H, J = 7.0 Hz), 3.59 (t, 2H, J = 6.7 Hz), 2.18 (qt, 2H, J = 7.0 Hz). ^{13}C NMR (100 MHz, acetone-d_6) δ: 181.7, 175.2, 167.3, 143.9, 134.1, 133.4, 131.9, 125.9, 122.2, 121.9, 46.9, 39.6, 34.3. Anal. Calcd for $C_{24}H_{18}ClN_5O_4$: C, 60.57; H, 3.81; N, 14.72. Found: C, 60.38; H, 3.69; N, 14.45.

4.2.4. 2-((4-(((3-Bromo-1,4-dioxo-1,4-dihydronaphthalen-2-yl)amino)methyl)-1*H*-1,2,3-triazol-1-yl)methyl)isoindoline-1,3-dione (20)

Using method C, compound **20** was obtained as a red solid (200 mg, 0.40 mmol, 88% yield); mp 155–157 °C. IR ν_{max} (cm^{-1}, KBr): 3250, 3123, 1778, 1725, 1675, 1596, 1567, 1401, 1361, 1329, 1292, 1132, 1045, 783, 737. ^{1}H NMR (400 MHz, acetone-d_6) δ: 8.13 (s, 1H), 8.07–7.65 (m, 8H), 7.02 (br s, 1H, NH), 6.25 (s, 2H), 5.20 (d, 2H, J = 5.1 Hz). ^{13}C NMR (100 MHz, acetone-d_6) δ: 179.4, 174.9, 165.9, 144.6, 134.4, 134.2, 131.9, 131.1, 130.9, 125.9, 122.9, 122.6, 49.4, 39.8. Anal. Calcd for $C_{22}H_{14}BrN_5O_4$: C, 53.68; H, 2.87; N, 14.23. Found: C, 53.62; H, 2.97; N, 13.86.

4.2.5. 2-(2-(4-(((3-Bromo-1,4-dioxo-1,4-dihydronaphthalen-2-yl)amino)methyl)-1*H*-1,2,3-triazol-1-yl)ethyl)isoindoline-1,3-dione (21)

Using method A, compound **21** was obtained as a red solid (200 mg, 0.40 mmol, 90% yield); mp 169–170 °C. IR ν_{max} (cm^{-1}, KBr): 3314, 3274, 3129, 1772, 1714, 1591, 1565, 1397, 1286, 1124, 1024, 939, 722. ^{1}H NMR (300 MHz, $CDCl_3$) δ: 8.14 (dd, 1H, J = 1.5 and 7.5 Hz), 8.03 (dd, 1H, J = 1.5 and 7.5 Hz), 7.79–7.77 (m, 2H), 7.76 (s, 1H), 7.72–7.61 (m, 4H), 6.48 (br s, 1H, NH), 5.14 (br s, 2H), 4.70 (t, 2H, J = 5.9 Hz), 4.15 (t, 2H, J = 5.9 Hz). ^{13}C NMR (100 MHz, $CDCl_3$) δ: 180.0, 176.5, 167.6, 146.2, 144.8, 134.7, 134.3, 132.5, 132.2, 131.6, 130.0, 127.0, 126.9, 123.6, 122.5, 48.2, 40.6, 37.7. Anal. Calcd for $C_{23}H_{16}BrN_5O_4$: C, 54.56; H, 3.19; N, 13.85. Found: C, 54.46; H, 3.58; H, 13.48.

4.2.6. 2-(3-(4-(((3-Bromo-1,4-dioxo-1,4-dihydronaphthalen-2-yl)amino)methyl)-1*H*-1,2,3-triazol-1-yl)propyl)isoindoline-1,3-dione (22)

Using method C, compound **22** was obtained as a red solid (200 mg, 0.40 mmol, 70% yield); mp 168–170 °C. IR ν_{max} (cm^{-1}, KBr): 3219, 3137, 1770, 1711, 1680, 1600, 1566, 1389, 1290, 1131, 1054, 715. ^{1}H NMR (300 MHz, $CDCl_3$) δ: 8.13 (dd, 1H, J = 0.9 and 6.9 Hz), 8.04 (dd, 1H, J = 1.2 and 7.5 Hz), 7.85–7.80 (m, 3H), 7.76–7.60 (m, 4H), 6.57 (br s, 1H, NH), 5.17 (d, 2H, J = 5.1 Hz), 4.41 (t, 2H, J = 6.6 Hz), 3.74 (t, 2H, J = 6.9 Hz), 2.35 (qt, 2H, J = 6.3 Hz). ^{13}C NMR (100 MHz, $CDCl_3$) δ: 180.2, 176.8, 168.6, 146.5, 135.0, 134.5, 132.8, 132.4, 132.1, 130.2, 127.3, 127.2, 123.7, 48.2, 40.9, 35.2, 29.6. Anal. Calcd for $C_{24}H_{18}BrN_5O_4$: C, 55.40, H, 3.49, N, 13.46. Found: C, 55.61, H, 3.82, N, 13.37.

4.2.7. 2-(((1-(3-Nitrophenyl)-1*H*-1,2,3-triazol-4-yl)methyl)amino)naphthalene-1,4-dione (23)

Using method B, compound **23** was obtained as an orange solid (200 mg, 0.54 mmol, 78% yield); mp 234–235 °C. IR ν_{max} (cm^{-1}, KBr): 3298, 3132, 1673, 1640, 1590, 1526, 1350, 1260, 1046, 804, 721. ^{1}H NMR (400 MHz, DMSO-d_6) δ: 8.94 (s, 1H), 8.68 (br s, 1H, NH), 8.38 (dd, 1H, J = 2.0 and 8.0 Hz), 8.30 (dd, 1H, J = 2.0 and 8.4 Hz), 8.02–7.71 (m, 6H), 5.80 (s, 1H), 4.62 (d, 2H, J = 4.8 Hz). ^{13}C NMR (100 MHz, DMSO-d_6) δ: 181.4, 181.3, 148.4, 148.1, 144.7, 137.0, 134.6, 132.9, 132.1, 131.3, 130.3, 125.9, 125.7, 125.2, 122.8, 121.7, 114.5, 100.6, 37.3. Anal. Calcd for $C_{19}H_{13}N_5O_4$: C, 60.80; H, 3.49; N, 18.66. Found: C, 60.83, H, 3.84, N, 18.86.

4.2.8. 2-Bromo-3-(((1-(3-nitrophenyl)-1*H*-1,2,3-triazol-4-yl)methyl)amino)naphthalene-1,4-dione (24)

Using method A, compound **24** was obtained as an orange solid (200 mg, 0.44 mmol, 86% yield); mp 175–176 °C. IR ν_{max} (cm^{-1}, KBr): 3298, 3132, 1673, 1640, 1590, 1526, 1350, 1260, 1046, 804, 721. ^{1}H NMR (400 MHz, DMSO-d_6) δ: 8.91 (s, 1H), 8.68 (br s, 1H, NH), 8.37 (d, 1H, J = 8.0 Hz), 8.29 (d, 1H, J = 8.4 Hz), 7.99 (d, 1H, J = 7.6 Hz), 7.88–7.74 (m, 5H), 5.16 (d, 2H, J = 6.4 Hz). ^{13}C NMR (100 MHz, DMSO-d_6) δ: 179.6, 175.3, 148.4, 147.4, 147.0, 137.1, 134.6, 132.6, 131.4, 131.3, 130.1, 126.5, 126.0, 125.8, 122.8, 121.3, 114.5. Anal. Calcd for $C_{19}H_{12}BrN_5O_4$, 0.45 × H_2O: C, 49.36; H, 2.81; N, 15.15. Found: C, 49.72; H, 3.18, N, 14.78.

4.2.9. 3-(4-(((1,4-Dioxo-1,4-dihydronaphthalen-2-yl)amino)methyl)-1*H*-1,2,3-triazol-1-yl)-2,2-dimethyl-2,3-dihydronaphtho[1,2-*b*]furan-4,5-dione (28)

Using method A, compound **28** was obtained as a yellow solid (220 mg, 0.7 mmol, 65% yield); mp 218–220 °C. IR ν_{max} (cm^{-1}, KBr): 3352 (NH), 1671 (C=O), 1654 (C=O), 1605 (C=O), 1565 (C=O). ^{1}H NMR (400 MHz, DMSO-d_6) δ: 8.26 (s, 1H), 8.02 (d, 1H, J = 7.34 Hz), 7.97–7.93 (m, 1H), 7.92–7.86 (m, 2H), 7.84–7.76 (m, 3H), 7.76–7.67 (m, 2H), 6.01 (s, 1H), 5.68 (s, 1H), 4.45 (d, 2H, J = 5.98 Hz), 1.65 (s, 3H), 0.97 (s, 3H). ^{13}C NMR (100 MHz, DMSO-d_6) δ: 181.9, 180.1, 174.9, 170.1, 148.6, 143.4, 135.2, 135.1, 133.4, 133.3, 132.7, 132.1, 130.7, 129.1, 126.9, 126.3, 125.7, 125.4, 123.9, 111.6, 101.0, 95.6, 66.5, 38.0, 27.3, 21.0. EI-HRMS (m/z) $[M+H]^+$: 481.1424. Calcd for $[C_{27}H_{20}N_4O_5H]^+$: 481.1512.

4.2.10. 3-(4-(((3-Bromo-1,4-dioxo-1,4-dihydronaphthalen-2-yl)amino)methyl)-1*H*-1,2,3-triazol-1-yl)-2,2-dimethyl-2,3-dihydronaphtho[1,2-*b*]furan-4,5-dione (29)

Using method A, compound **29** was obtained as an orange solid 196 mg, 0.5 mmol, 70% yield); mp 167–168 °C. IR ν_{max} (cm^{-1}, KBr): 3348 (NH), 1671 (C=O), 1651 (C=O), 1608 (C=O), 1565 (C=O). ^{1}H NMR (400 MHz, DMSO-d_6) δ: 8.21 (s, 1H), 8.01 (d, 1H, J = 7.26 Hz), 7.94–7.88 (m, 2H), 7.84–7.75 (m, 3H), 7.74–7.68 (m, 3H), 5.99 (s, 1H), 4.99 (d, 2H, J = 6.36 Hz), 1.65 (s, 3H), 0.97 (s, 3H). ^{13}C NMR (100 MHz, DMSO-d_6) δ: 180.1, 175.8, 174.9, 170.2, 168.7, 147.2, 145.6 135.1, 133.4, 133.1, 132.1, 131.8, 130.4, 129.1, 127.0, 126.4, 125.4, 123.4, 123.3, 111.7, 95.6, 40.3, 27.3, 21.0. EI-HRMS (m/z) $[M+H]^+$: 559.0532. Calcd for $[C_{27}H_{19}BrN_4O_5H]^+$: 559.0617.

4.2.11. 3-(4-(((3-Chloro-1,4-dioxo-1,4-dihydronaphthalen-2-yl)amino)methyl)-1*H*-1,2,3-triazol-1-yl)-2,2-dimethyl-2,3-dihydronaphtho[1,2-*b*]furan-4,5-dione (30)

Using method A, compound **30** was obtained as an orange solid (211 mg, 0.5 mmol, 82% yield); mp 194–195 °C. IR ν_{max} (cm^{-1}, KBr): 3355 (NH), 1671 (C=O), 1615 (C=O), 1605 (C=O), 1565 (C=O). ^{1}H NMR (400 MHz, DMSO-d_6) δ: 8.24 (s, 1H), 8.02 (d, 1H, J = 6.94 Hz), 7.95–7.90 (m, 2H), 7.86–7.76 (m, 4H), 7.76–7.70 (m, 2H), 6.02 (s, 1H), 4.98 (d, 2H, J = 6.65 Hz), 1.67 (s, 3H), 0.99 (s, 3H). ^{13}C NMR (100 MHz, DMSO-d_6) δ: 180.4, 180.2, 175.9, 174.9,

170.1, 145.8, 135.3, 135.1, 133.4, 133.2, 132.1, 132.1, 130.3, 129.1, 127.0, 126.9, 126.2, 125.4, 123.3, 111.7, 95.6, 66.5, 40.3, 27.3, 21.0. EI-HRMS (*m*/*z*) $[M+H]^+$: 515.1022. Calcd for $[C_{27}H_{19}ClN_4O_5H]^+$: 515.1122.

4.2.12. 2,2-Dimethyl-3-(4-phenyl-1*H*-1,2,3-triazol-1-yl)-2,3-dihydrobenzo[*f*]furo[2,3-*h*]quinoxaline (36)

Nor-β-lapachone-based 1,2,3-triazole **31** (200 mg, 0.54 mmol) was reacted with an excess of ethylenediamine (65 mg, 1.08 mmol) in 30 mL toluene. The reaction was stirred under reflux in a Dean–Stark apparatus till the total consumption of the reagents as monitored by TLC. The solvent was evaporated under reduced pressure. The residue obtained was purified by column chromatography on silica gel using an increasing polarity mixture of hexane/ethyl acetate as eluent. Compound **36** was obtained as a yellow solid (162 mg, 0.41 mmol, 77% yield, mp 235–238 °C); IR (KBr) 1595 (C=N), 1346 (C=C), 1070 (C–O), 767 (C–H) cm^{-1}. ^1H NMR (400 MHz, $CDCl_3$) δ: 9.28 (dd, 1H, J = 8.11 and 0.73 Hz), 8.74 (d, 1H, J = 2.16 Hz), 8.67 (d, 1H, J = 2.16 Hz), 8.25 (dd, 1H, J = 7.86 and 0.89 Hz), 7.95–7.84 (m, 2H), 7.71–7.67 (m, 2H), 7.34–7.28 (m, 2H), 7.26–7.22 (m, 2H), 6.63 (s, 1H), 1.80 (s, 3H), 1.34 (s, 3H). ^{13}C NMR (100 MHz, $CDCl_3$) δ: 158.1, 146.1, 144.9, 141.0, 140.6, 138.2, 132.3, 130.3, 129.6, 129.5, 129.0, 128.8, 127.9, 125.2, 125.1, 124.7, 122.6, 122.5, 121.5, 109.8, 92.2, 67.7, 27.0, 21.1.

4.2.13. 2,2-Dimethyl-1-(4-phenyl-1*H*-1,2,3-triazol-1-yl)-1,2-dihydrobenzo[*a*]furo[2,3-*c*]phenazine (37)

Nor-β-lapachone-based 1,2,3-triazole **31** (150 mg, 0.4 mmol) was reacted with *ortho*-phenylenediamine (41 mg, 0.44 mmol) and sodium acetate (62 mg, 0.76 mmol) in 25 mL glacial acetic acid. The reaction was stirred at room temperature for 2 h. The reaction was shed over cold water and the precipitate filtered using Buchner funnel. The solid obtained was purified by column chromatography on silica gel using an increasing polarity mixture of hexane/ethyl acetate as eluent. Compound **37** was obtained as a yellow solid (195 mg, 0.44 mmol, 82% yield, mp 224–227 °C); IR (KBr) 1597 (C=N), 1346 (C=C), 1049 (C–O), 763 (C–H) cm^{-1}.^1H NMR (400 MHz, $CDCl_3$) δ: 9.48 (d, 1H, J = 8.16 Hz), 8.31–8.26 (m, 1H), 8.26–8.21 (m, 1H), 8.06–8.01 (m, 1H), 7.98–7.93 (m, 1H), 7.92–7.86 (m, 1H), 7.78–7.72 (m, 2H), 7.70–7.66 (m, 2H), 7.31–7.25 (m, 3H), 7.24–7.18 (m, 1H), 6.73 (s, 1H), 1.83 (s, 3H), 1.36 (s, 3H). ^{13}C NMR (100 MHz, DMSO-d_6) δ: 160.2, 146.6, 142.2, 142.2, 141.1, 139.9, 132.9, 131.2, 131.0, 130.8, 130.5, 129.8, 129.6, 129.2, 129.1, 129.1, 128.6, 126.1, 125.5, 125.4, 124.3, 123.5, 121.8, 109.4, 93.1, 68.2, 27.5, 21.6.

4.2.14. (*Z*)-5-(Hydroxyimino)-2,2-dimethyl-3-(4-phenyl-1*H*-1,2,3-triazol-1-yl)-2,3-dihydronaphtho[1,2-*b*]furan-4(5*H*)-one (38)

Nor-β-lapachone-based 1,2,3-triazole **31** (200 mg, 0.54 mmol) was reacted with hydroxylamine hydrochloride (120 mg, 1.68 mmol), sodium acetate (89 mg, 1.08 mmol) and catalytic triethylamine in 30 mL methanol. The reaction was stirred under reflux overnight. The solvent was evaporated under reduced pressure. The residue obtained was purified by column chromatography on silica gel using an increasing polarity mixture of hexane/ethyl acetate as eluent. Compound **38** was obtained as a yellow solid (129 mg, 0.33 mmol, 62% yield, mp 222–225 °C); IR (KBr) 3449 (OH), 1609 (C=O), 1524 (C=N), 972 (N–O) cm^{-1}. ^1H NMR (400 MHz, $CDCl_3$) δ: 8.41 (d, 1H, J = 8.09 Hz), 7.90 (d, 1H, J = 7.75 Hz), 7.81 (d, 2H, J = 7.55 Hz), 7.73 (t, 1H, J = 7.67 Hz), 7.66–7.58 (m, 2H), 7.40 (t, 2H, J = 7.53 Hz), 7.32 (t, 1H, J = 7.53 Hz), 6.10 (s, 1H), 1.78 (s, 3H), 1.27 (s, 3H). ^{13}C NMR (100 MHz, $CDCl_3$) δ: 202.5, 170.9, 149.4, 147.0, 131.7, 129.7, 129.6, 128.9, 128.8, 128.5, 126.2, 126.0, 125.1, 123.3, 123.3, 123.1, 118.7, 103.0, 89.9, 60.3, 23.1, 23.1.

4.4. Trypanocidal activity

Stock solutions of the compounds were prepared in dimethyl sulfoxide (DMSO), with the final concentration of the latter in the experiments never exceeding 0.1%. Preliminary experiments showed that concentrations of up to 0.5%, DMSO have no deleterious effect on the parasites. Bloodstream trypomastigotes of the Y strain were obtained at the peak of parasitaemia from infected albino mice, isolated by differential centrifugation and resuspended in Dulbecco's modified Eagle medium (DME) to a parasite concentration of 10^7 cells/mL in the presence of 10% of mouse blood. This suspension (100 μL) was added in the same volume of each compound previously prepared at twice the desired final concentrations. Cell counts were performed in Neubauer chamber and the trypanocidal activity was expressed as IC_{50}, corresponding to the concentration that leads to lysis of 50% of the parasites.

4.5. Toxicity to heart muscle cells

The cytotoxicity assays were performed using primary cultures of heart muscle cells (HMC). Briefly, hearts of 18-day-old mouse embryos were fragmented and dissociated with trypsin and collagenase in phosphate buffered saline (PBS pH 7.2), as previously established.[33] For these experiments, 6×10^4 cardiomyocytes in 100 mL of RPMI-1640 medium (pH 7.2) plus 10% foetal bovine serum and 2 mM glutamine were added to each well of a 96-well microtiter plate and incubated for 24 h at 37 °C. The treatment with **28**–**30** was performed in fresh supplemented medium without phenol red (200 μL/well) for 24 h at 37 °C. After this period, 110 μL of the medium was discarded and 10 μL of PrestoBlue (Invitrogen) was added to complete the final volume of 100 μL. Thus, the plate was incubated for 5 h and the measurement was performed at 570 and 600 nm, as recommended by the manufacturer. The results were expressed as the difference in the percentage of reduction between treated and untreated cells being the LC_{50} value, corresponds to the concentration that leads to damage of 50% of the mammalian cells.

4.6. X-ray analysis

X-ray data were collected at 150 K using MoKα (0.71073 Å) on an Agilent—Gemini diffractometer equipped with a CCD area detector. The CrysAlisPro software package[34] was used for data collection and data reduction. The data were corrected empirically for absorption using spherical harmonics using the SCALE3 ABSPACK[35] scaling algorithm. The structure was solved by direct methods using SHELXS-97[36] and refined by full-matrix least squares on F^2 using SHELXL-97.[37] All non-hydrogen atoms were successfully refined using anisotropic displacement parameters. Hydrogen atoms were found in the Fourier difference synthesis and fixed. Crystallographic data for the structure were deposited in the Cambridge Crystallographic Data Centre, with number CCDC 926844.

4.7. Electrochemical studies

Cyclic voltammetry (CV) experiments were performed with a conventional undivided three electrode cell using an Autolab PGSTAT-30 potentiostat (Echo Chemie, Utrecht, the Netherlands) coupled to a microcomputer, interfaced by GPES 4.9 software. Glassy carbon (GC) (diameter = 3 mm) as the working electrode, a Pt wire as the counter electrode and the reference electrode an Ag|AgCl, Cl^- (saturated) were used. The GC electrode was cleaned up by polishing with alumina on a polishing felt (BAS polishing kit). The solvent used in aprotic media studies, DMF, was distilled under reduced pressure after stirring with anhydrous copper sulfate. In CV experiments, the scan rate varied from 10 to 500 mV

s^{-1}. All experiments were conducted at room temperature (25 ± 2 °C) and purging an inert gas (Argon). Electrochemical reduction in aprotic media (DMF + TBAP 0.1 mol L^{-1}) was performed in the absence of oxygen. Each compound (1×10^{-3} mol L^{-1}) was added to the supporting electrolyte and the solution was deoxygenated with argon before the measurements by cyclic voltammetry.

4.8. Statistical analysis

The comparison between the IC_{50} values for *T. cruzi* was performed by ANOVA followed by the Student–Newman–Keuls and Mann–Whitney tests (p <0.05).

Acknowledgments

This research was funded by grants from the Conselho Nacional de Desenvolvimento Científico e Tecnológico (CNPq) Project Universal—MCTI/CNPq no 14/2012 (480719/2012-8), FAPEMIG APQ-04166-10, PRONEM-FACEPE (1232.1.06/10), CENAPESQ-UFRPE, PRONEX/FAPEAL/CNPq and CAPES. Dr. E.N. da Silva Júnior also thanks the Programa Institucional de Auxílio à Pesquisa de Doutores Recém-Contratados and Universidade Federal de Minas Gerais. The authors would like to thank Professors Bruno C. Cavalcanti and Claudia Pessoa for the support with the biological assays.

References and notes

1. Rassi Júnior, A.; Rassi, A.; Rezende, J. M. *Infect. Dis. Clin. North Am.* **2012**, *26*, 275.
2. Schofield, C. J.; Jannin, J.; Salvatella, R. *Trends Parasitol.* **2006**, *22*, 583.
3. Shikanai-Yasuda, M. A.; Carvalho, N. B. *Clin. Infect. Dis.* **2012**, *54*, 845.
4. Coura, J. R.; Junqueira, A. C. *Mem. Inst. Oswaldo Cruz* **2012**, *107*, 145.
5. Schmunis, G. A.; Yadon, Z. E. *Acta Trop.* **2010**, *115*, 14.
6. Coura, J. R.; Viñas, P. A. *Nature* **2010**, *465*, S6.
7. Dias, J. C. P.; Prata, A.; Correia, D. *Rev. Soc. Bras. Med. Trop.* **2008**, *41*, 193.
8. Abad-Franch, F.; Santos, W. S.; Schofield, C. J. *Acta Trop.* **2010**, *115*, 44.
9. Guedes, P. M. M.; Silva, G. K.; Gutierrez, F. R. S.; Silva, J. S. *Expert Rev. Anti Infect. Ther.* **2011**, *9*, 609.
10. Soeiro, M. N. C.; de Castro, S. L. *Open Med. Chem. J.* **2011**, *5*, 21.
11. DNDi 2012 New letter Chagas Disease Clinical Research Platform, dez 2012 http://www.dndi.org.br/images/stories/img_videos/NEWSLETTERChagasEd2%20(1)(1).pdf, accessed 12/6/2012.
12. (a) Salas, C. O.; Faúndez, M.; Morello, A.; Maya, J. D.; Tapia, R. A. *Curr. Med. Chem.* **2011**, *18*, 144; (b) Pieretti, S.; Haanstra, J. R.; Mazet, M.; Perozzo, R.; Bergamini, C.; Prati, F.; Fato, R.; Lenaz, G.; Capranico, G.; Brun, R.; Bakker, B. M.; Michels, P. A. M.; Scapozza, L.; Bolognesi, M. L.; Cavalli, A. *PLoS Negl. Trop. Dis.* **2013**, *7*, e2012.
13. O'Brien, P. J. *Chem. Biol. Interact.* **1991**, *80*, 1.
14. Constantino, L.; Barlocco, D. *Curr. Med. Chem.* **2006**, *13*, 65.
15. Pinto, A. V.; de Castro, S. L. *Molecules* **2009**, *14*, 4570.
16. (a) da Silva Júnior, E. N.; Menna-Barreto, R. F. S.; Pinto, M. C. F. R.; Silva, R. S. F.; Teixeira, D. V.; Souza, M. C. B. V.; de Simone, C. A.; de Castro, S. L.; Ferreira, V. F.; Pinto, A. V. *Eur. J. Med. Chem.* **2008**, *43*, 1774; (b) da Silva Júnior, E. N.; Guimarães, T. T.; Menna-Barreto, R. F. S.; Pinto, M. C. F. R.; de Simone, C. A.; Pessoa, C.; Cavalcanti, B. C.; Sabino, J. R.; Andrade, C. K. Z.; Goulart, M. O. F.; de Castro, S. L.; Pinto, A. V. *Bioorg. Med. Chem.* **2010**, *18*, 3224; (c) da Silva Júnior, E. N.; de Moura, M. A. B. F.; Pinto, A. V.; Pinto, M. C. F. R.; Souza, M. C. B. V.; Araújo, A. J.; Pessoa, C.; Costa-Lotufo, L. V.; Montenegro, R. C.; de Moraes, R. C.; Goulart, M. O. F.; Ferreira, V. F. *J. Braz. Chem. Soc.* **2009**, *20*, 635; (d) da Silva Júnior, E. N.; Melo, I. M. M.; Diogo, E. B. T.; Costa, V. A.; Souza Filho, J. D.; Valença, W. O.; Camara, C. A.; Oliveira, R. N.; Araujo, A. S.; Emery, F. S.; Santos, M. R.; de Simone, C. A.; Menna-Barreto, R. F. S.; de Castro, S. L. *Eur. J. Med. Chem.* **2012**, *52*, 304.
17. (a) Guimarães, T. T.; Pinto, M. C. F. R.; Lanza, J. S.; Melo, M. N.; do Monte-Neto, R. L.; de Melo, I. M. M.; Diogo, E. B. T.; Ferreira, V. F.; Camara, C. A.; Valença, W. O.; de Oliveira, R. N.; Frézard, F.; da Silva Júnior, E. N. *Eur. J. Med. Chem.* **2013**, *63*, 523; (b) Rostovtsev, V. V.; Green, G. L.; Fokin, V. V.; Sharpless, K. B. *Angew. Chem., Int. Ed.* **2002**, *41*, 2596.
18. (a) Pinto, A. V.; Neves Pinto, C.; Pinto, M. C. F. R.; Santa Rita, R.; Pezzella, C. A. C.; de Castro, S. L. *Arzneim.-Forsch.* **1997**, *47*, 74; (b) Neves Pinto, C.; Dantas, A. P.; Moura, K. C. G.; Emery, F. S.; Polequevitch, P. F.; Pinto, M. C. F. R.; de Castro, S. L.; Pinto, A. V. *Arzneim.-Forsch.* **2000**, *50*, 1120; (c) Pinto, A. V.; Cruz, F. S.; Pellegrino, J.; Mello, R. T. *Trans. Roy. Soc. Trop. Med. Hyg.* **1977**, *71*, 133; (d) da Silva Júnior, E. N.; de Souza, M. C. B. V.; Fernandes, M. C.; Menna-Barreto, R. F. S.; Pinto, M. C. F. R.; Lopes, F. A.; de Simone, C. A.; Andrade, C. K. Z.; Pinto, A. V.; Ferreira, V. F.; de Castro, S. L. *Bioorg. Med. Chem.* **2008**, *16*, 5030.
19. (a) Goulart, M. O. F.; Zani, C. L.; Tonholo, J.; Freitas, L. R.; de Abreu, F. C.; Oliveira, A. B.; Raslan, D. S.; Starling, S.; Chiari, E. *Bioorg. Med. Chem. Lett.* **1997**, *7*, 2043; (b) Paulino, M.; Alvareda, E. M.; Denis, P. A.; Barreiro, E. J.; Sperandio da Silva, G. M.; Dubin, M.; Gastellú, C.; Aguilera, S.; Tapia, O. *Eur. J. Med. Chem.* **2008**, *43*, 2238; (c) Pérez-Silanes, S.; Devarapally, G.; Torres, E.; Moreno-Viguri, E.; Aldana, I.; Monge, A.; Crawford, P. W. *Helv. Chim. Acta* **2013**, *96*, 217.
20. Song, Y.; Buettner, G. R. *Free Radical Biol. Med.* **2010**, *49*, 919.
21. (a) Hillard, E. A.; de Abreu, F. C.; Ferreira, D. C. M.; Jaouen, G.; Goulart, M. O. F.; Amatore, C. *Chem. Commun.* **2008**, 2612; (b) Araújo, A. J.; de Souza, A. A.; da Silva Júnior, E. N.; Marinho Filho, J. D. B.; de Moura, M. A. B. F.; Rocha, D. D.; Vasconcellos, M. C.; Costa, C. O.; Pessoa, C.; de Moraes, M. O.; Ferreira, V. F.; de Abreu, F. C.; Pinto, A. V.; Montenegro, R. C.; Costa-Lotufo, L. V.; Goulart, M. O. F. *Toxicol In Vitro* **2012**, *26*, 585; (c) Cavalcanti, B.; Barros, F. W. A.; Cabral, I.; Ferreira, J.; Magalhães, H.; Júnior, H.; da Silva Júnior, E. N.; de Abreu, F. C.; Costa, C. O.; Goulart, M. O. F.; Moraes, M. O.; Pessoa, C. *Chem. Res. Toxicol.* **2011**, *24*, 1560; (d) Ferreira, D. C. M.; Tapsoba, I.; Arbault, S.; Bouret, Y.; Moreira, A. M. S.; Pinto, A. V.; Goulart, M. O. F.; Amatore, C. *ChemBioChem* **2009**, *10*, 528.
22. Ceric, H.; Šindler-Kulyk, M.; Kovacevic, M.; Peric, M.; Ivkovic, A. Z. *Bioorg. Med. Chem.* **2010**, *18*, 3053.
23. Spallarossa, A.; Cesarini, S.; Ranise, A.; Bruno, O.; Schenone, S.; La Colla, P.; Collu, G.; Sanna, G.; Secci, B.; Loddo, R. *Eur. J. Med. Chem.* **2009**, *44*, 1650.
24. Banik, B. K.; Banik, I.; Becker, F. F. *Bioorg. Med. Chem.* **2005**, *13*, 3611.
25. Li, Y. F.; Wang, G. F.; He, P. L.; Huang, W. G.; Zhu, F. H.; Gao, H. Y.; Tang, W.; Luo, Y.; Feng, C. L.; Shi, L. P.; Ren, Y. D.; Lu, W.; Zuo, J. P. *J. Med. Chem.* **2006**, *49*, 4790.
26. Fieser, L. F.; Fieser, M. *J. Am. Chem. Soc.* **1948**, *70*, 3215.
27. da Silva, M. T.; de Oliveira, R. N.; Valença, W. O.; Barbosa, F. C. G.; da Silva, M. G.; Camara, C. A. *J. Braz. Chem. Soc.* **2012**, *23*, 1839.
28. Hein, J. E.; Fokin, V. V. *Chem. Soc. Rev.* **2010**, *39*, 1302.
29. Meldal, M.; Tornøe, C. W. *Chem. Rev.* **2008**, *108*, 2952.
30. Silva, R. S. F.; Pinto, M. C. F. R.; Goulart, M. O. F.; de Souza Filho, J. D.; Neves Júnior, I.; Lourenço, M. C. S.; Pinto, A. V. *Eur. J. Med. Chem.* **2009**, *44*, 2334.
31. Emery, F. S.; Silva, R. S. F.; de Moura, K. C. G.; Pinto, M. C. F. R.; Amorim, M. B.; Malta, V. R. S.; Santos, R. H. A.; Honório, K. M.; da Silva, A. B. F.; Pinto, A. V. *An. Acad. Bras. Cienc.* **2007**, *79*, 29.
32. Romanha, A. J.; de Castro, S. L.; Soeiro, M. N.; Lannes-Vieira, J.; Ribeiro, I.; Talvani, A.; Bourdin, B.; Blum, B.; Olivieri, B.; Zani, C.; Spadafora, C.; Chiari, E.; Chatelain, E.; Chaves, G.; Calzada, J. E.; Bustamante, J. M.; Freitas-Júnior, L. H.; Romero, L. I.; Bahia, M. T.; Lotrowska, M.; Soares, M.; Andrade, S. G.; Armstrong, T.; Degrave, W.; Andrade, Z. A. *Mem. Inst. Oswaldo Cruz* **2010**, *105*, 233.
33. Meirelles, M. N.; de Araujo-Jorge, T. C.; Miranda, C. F.; de Souza, W.; Barbosa, H. S. *Eur. J. Cell Biol.* **1986**, *41*, 198.
34. *CRYSALISPRO*, Agilent Technologies, Version 1.171.35.21 (release 20-01-2012 CrysAlis171.NET.
35. *SCALE3 ABSPACK Scaling Algorithm*. CrysAlis, Agilent Technologies, Version 1.171.35.21 (release 20-01-2012 CrysAlis171.NET).
36. Sheldrick, G. M. SHELXS-*97 Program for the Solution of Crystal Structures*; University of Göttingen: Germany, 1997.
37. Sheldrick, G. M. SHELXS-*97, Program for the Refinement of Crystal Structures*; University of Göttingen: Germany, 1997.